Solar Energy 165 (2018) 122–130

Contents lists available at ScienceDirect

Solar Energy

journal homepage: www.elsevier.com/locate/solener

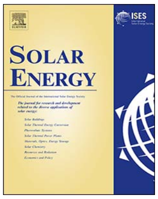

Improving the photovoltaic performance of Zn_2SnO_4 solar cells by doping Sr^{2+}/Ba^{2+} ions: Efficient electron injection and transfer

Jie Dou[a,b], Yafeng Li[a,b,*], Junxiu Wu[a,b], Yuan Jay Chang[c], Mingdeng Wei[a,b,*]

[a] State Key Laboratory of Photocatalysis on Energy and Environment, Fuzhou University, Fuzhou, Fujian 350002, China
[b] Institute of Advanced Energy Materials, Fuzhou University, Fuzhou, Fujian 350002, China
[c] Department of Chemistry, Tunghai University, Taichung 40704, Taiwan

ARTICLE INFO

Keywords:
Photovoltaic performance
Zn_2SnO_4
Doping
Band gap energy

ABSTRACT

In the present study, the nanocrystalline Zn_2SnO_4 dopen with Sr^{2+}/Ba^{2+} ions is synthesized via a hydrothermal method and their structure is analyzed in detail. Moreover, the photovoltaic properties of dye-sensitized solar cells composed of doped Zn_2SnO_4 are investigated. The enlarged energy difference between the conduction band edge of Zn_2SnO_4 and the lowest unoccupied molecular orbit (LUMO) of dye gives rise to the enhanced driving force for electron injection. The DSCs based on Sr^{2+}/Ba^{2+} doped Zn_2SnO_4 improve the power efficiency through enhancing charge transport processes and reducing recombination rates. Compared to the photovoltaic conversion efficiency of pure Zn_2SnO_4 cells, the DSCs based on ZTO-Sr (3.0) exhibit a greater power conversion efficiency of 4.91%. As a consequence, the device of ZTO-Ba (1.5) also demonstrates an improved efficiency of up to 4.94%. This corresponds to an enhancement in power conversion efficiency of 17%, respectively, relative to control devices.

1. Introduction

Due to low cost, simple fabrication process and high photovoltaic efficiency, a mass of attention has been paid to dye-sensitized solar cells (DSCs). The DSCs consist of three main parts: a dye-sensitized semiconductor with suitable band gap energy printed on FTO substrate, a liquid or solid electrolyte comprising redox couple pair, and a high catalytic activity counter electrode. As a key factor impact on the photovoltaic performance of DSCs, the optimization of the photoanode materials is still one of the important research targets. In spite of binary metal oxides, such as TiO_2 (Guo et al., 2017; Zhong et al., 2015), ZnO (Kunzmann et al., 2016) and SnO_2 (Snaith and Ducati, 2010), are widely applied as electrode materials, ternary metal oxides (Zn_2SnO_4 Wang et al., 2013, $BaSnO_3$ (Shin et al., 2013), $SrSnO_3$ (Li et al., 2012), etc.) have emerged as promising alternatives in recent years. Especially, as a broader choice of materials, Zn_2SnO_4 photoanodes have attracted wide attention on account of their intrinsic advantages. Firstly, Zn_2SnO_4 films feature the higher electron mobility (10–15 $cm^2\ V^{-1}\ s^{-1}$) and the wider band gap (3.6 eV) relative to TiO_2 films (Wang et al., 2013). Secondly, the electron injection and recombination dynamics are similar for both binary and ternary oxides based electrodes under comparable operation conditions, which is beneficial for enhancing the efficiency of DSCs based on Zn_2SnO_4 nanoparticles. The band structures of Zn_2SnO_4 are easier to be regulated and controlled compared to TiO_2. Recently, Kuang group (Wang et al., 2013) reported the DSCs based on Zn_2SnO_4 nanoparticles exhibited the power conversion efficiency (PCE) of 4.01%, and then improved the efficiency by using hydrothermally fabricated macroporous Zn_2SnO_4. In addition, Kim et al. Hwang et al. (2014) fabricated hierarchically structured Zn_2SnO_4 nanobeads, and the unique morphology of the Zn_2SnO_4 improved the light scattering. However, one of the major disadvantages of Zn_2SnO_4 based DSCs are their prominent electron loss process, which influence the electron lifetime and electron transport time throughout the electrode, resulting in the poor charge collection efficiencies.

To tackle these problems, the surface treatment, the fabrication of different nanostructures and calcination treatment have been known to be valid ways in increasing photovoltaic performance of Zn_2SnO_4-based DSCs using. In 2014, the surface treatment with Zn or Sn precursor solutions is firstly applied for improving the photovoltaic performance of dye-sensitized Zn_2SnO_4 solar cell by reducing the density of surface traps. (Chen et al., 2014) Furthermore, the photovoltaic performance might be enhanced by doping, which can shift the semiconductor energy edge and improve electron collection efficiency. For example, the improved charge transport and reduced recombination rates were realized by using In-doped zinc oxide (Kunzmann et al., 2016). The Nb doping in TiO_2 gave rise to a significant increase of powder

---

[*] Corresponding authors at: State Key Laboratory of Photocatalysis on Energy and Environment, Fuzhou University, Fuzhou, Fujian 350002, China.
E-mail addresses: liyf@fzu.edu.cn (Y. Li), wei-mingdeng@fzu.edu.cn (M. Wei).

https://doi.org/10.1016/j.solener.2018.03.012
Received 16 November 2017; Received in revised form 1 March 2018; Accepted 5 March 2018

conductivity and a positive shift in the V_{fb} (Lü et al., 2010). However, the doping on binary oxides is restricted by the radius difference between metal cations, and the introduction of dopant might result in the formation of other compounds instead of the case of doping. The employment of Sr^{2+} cations into TiO_2 electrodes led to the appearance of $SrTiO_3$ rather than Sr-doped TiO_2 (Diamant et al., 2003). By contrast, ternary oxides are believed to have more doping sites and better structural tolerance. Co- or Mn-doped Zn_2SnO_4 nanowires were reported as a promising ternary oxide for room temperature ferromagnetism (Deng et al., 2013; Sumithra and Victor Jaya, 2016). Zn_2SnO_4 has been known as a prospective photovoltaic response material on doping with Eu^{3+}, Bi^{3+} and Dy^{3+} cations (Dimitrievska et al., 2016; Liu et al., 2013; Wang et al., 2007). In a previous study, our group improved the efficiency of DSCs cell by a facile chemical-bath deposition method, where Al^{3+} cations were introduced into the lattice of Zn_2SnO_4, bringing about reduced conduction band edge. (Li et al., 2011; Dou et al., 2017) Nevertheless, there is no direct study on the doping of ternary oxides with metal cations having dramatically larger radius to demonstrate that the ternary oxides are “in deed” more susceptible to doping in comparison to binary oxides up to now. Herein, the Sr^{2+} and Ba^{2+} cations are used to dope Zn_2SnO_4 nanoparticles by using a hydrothermal method as a case study on doping ternary oxides by metal cations with notably different radius. The ion radius of Sr^{2+}, Ba^{2+}, Zn^{2+} and Sn^{4+} are 1.18, 1.35, 0.74 and 0.69 Å, respectively. Although the radius of dopants employed here are significantly larger than those in Zn_2SnO_4, the results denoted that both of Sr^{2+} and Ba^{2+} cations could be easily doped into the lattice of Zn_2SnO_4. Moreover, their xinfluence on the photovoltaic performance of Zn_2SnO_4-based cells is systematically studied.

2. Experimental

2.1. Materials preparation and measurements

In a classic synthesis, 1.5 mmol potassium stannate ($K_2SnO_3{\cdot}3H_2O$) was added to the mixed solvents composing 10 mL ethylene glycol and 30 mL deionized water. And then different amounts of $Sr(CH_3COO)_2{\cdot}0.5H_2O$ or $Ba(CH_3COO)_2$ and 3 mmol zinc acetate ($Zn(CH_3COO)_2{\cdot}2H_2O$) was added to the mixed solution under strongly stirring, subsequently. After that 1 mL ammonia was dropwise added to the mixed solution and paid attention to the stirring and then the mixture was shifted to a 100 mL Teflon-lined autoclave and heated to 200 °C for 24 h. After cooling down, the sediment was received by centrifugation, and washed by DI water, ethyl alcohol and 1 mM HCl, subsequently. Ultimately, the powder was dried at 70 °C for 12 h and calcined at 450 °C for 3 h. As a reference sample, pure Zn_2SnO_4 nanoparticles were prepared in the same route without adding $Sr(CH_3COO)_2{\cdot}0.5H_2O$ or $Ba(CH_3COO)_2$.

The samples were characterized by X-ray diffraction (Rigaku, CuKα, λ = 1.5418 Å), scanning electron microscope (Hitachi, S4800), transmission electron microscope (FEI, Tecnai G^2 F20), Surface Area Analyzer (Micromeritics, ASAP 2020), X-ray photoelectron spectroscopy (Thermo Electron, Multilab 2000) and Inductively Coupled Plasma-Atomic Emission spectrometry (Perkin-Elmer, OPTIMA 8000). UV–vis absorption spectra were measured by a UV-2450.

2.2. Dscs fabrication and photovoltaic performance measurements

Through the screen printing method on 14 Ω/sq^2 FTO, fabrication of the DSCs was carried out using the sample with 10 wt% ethyl cellulose as the agglomerant, 5 wt% α-terpineol and 120 mL absolute ethanol, followed by calcination at 525 °C for 120 min. Those films were immersed into the solution including 0.3 mM N719 dye, 0.3 mM D131 dye and 6 mM deoxycholic acid in isopropyl alcohol and acetonitrile (Visopropyl alcohol : Vacetonitrile = 1:1) for 6 h. The counter electrode was provided by means of dropping 5 mM H_2PtCl_6 solution on the FTO followed closely by calcination at 400 °C for 15 min. In order to hinder the cell from short circuit, the polyethylene spacer possessing a film thickness of 38 μm was placed between the counter electrode and the working electrode. The component of electrolyte are 50 mM I_2, 100 mM LiI, and 60 mM 1,2-dimethyl-3-n-propylimidazolium iodide and 1 M 4-tertbutylpyridine in acetonitrile. The effective area of the electrode films was 25 mm^2.

The performance of the DSCs was characterized on the source meter (Keithley 2400). The PEC-L11 AM 1.5 solar simulator (Peccell, Xe lamp) was applied as the light source (100 mW cm^{-2}). The IPCE spectra were recorded by the PEC-S20 (Peccell). Under a modulated blue light emitting diodes (457 nm) supplied by a Zahner (PP211) source, the IMVS and IMPS were measurement by the electrochemical workstation (Zahner, IM6) using a frequency response analyzer. Mott–Schottky plots and Open-circuit photovoltage decay spectra were both recorded by the electrochemical workstation (Zahner, IM6). The film thickness was measured through Surfcom 130 A.

3. Results and discussion

To distinguish the different samples, the pure Zn_2SnO_4 nanoparticles are labeled as ZTO, and ZTO-Sr and ZTO-Ba denote the Zn_2SnO_4 nanoparticles are doped by Sr^{2+} or Ba^{2+} cations, while the number following ZTO-Sr or ZTO-Ba means the mini mole number of dopant added in the preparation process. The XRD patterns of some typical samples were measured and revealed in Fig. 1. As can be seen from Fig. 1, all of the diffraction peaks are in great agreement with the Zn_2SnO_4 (JCPDS 74-2184) and no impurities could be found. The peaks at 2θ of 17.7°, 29.2°, 34.3°, 35.9°, 41.7°, 55.1° and 60.5° correspond to the (1 1 1), (2 2 0), (3 1 1), (2 2 2), (4 0 0), (5 1 1) and (4 4 0) crystal planes of Zn_2SnO_4 (space group Fd-3 m (O_h^7)), respectively. The results in Fig. 1c and d suggests the peak locates between 34.0° and 34.5° slightly shifts to lower angles due to the doping of Sr^{2+} and Ba^{2+} cations. As shown in Fig. S1, the peak shape was perfectly symmetrical with the doping of Sr^{2+} and Ba^{2+} cations. According to the fitting curve, there were no impure peaks that may be caused by the doping of Sr^{2+} and Ba^{2+} cations. Moreover, the shift of the peak becomes more obvious when the doping amounts were increased, implying the successful doping of Sr^{2+} and Ba^{2+} cations into the lattice of Zn_2SnO_4.

Zn_2SnO_4 crystals has a spinel structure accompanied by 96 cation sites per unit cell in which 24 of the sites are occupied by Zn^{2+} or Sn^{4+} cations. This creates abundant of unoccupied sites. Besides, the degree of cation disorder which is recorded to be more than 30% is also beneficial for creation of more number of defects (Deng et al., 2013). The crystal structure obtained from the Rietveld refinement of the XRD pattern for the samples compound is presented in Fig. 1. After doping with Sr^{2+} cations, an increase of a-axis lattice constant from 8.677 to 8.680 Å was observed for sample ZTO-Sr (3.0), implying that some Sr^{2+} cations may occupy Zn^{2+} or Sn^{4+} sites in the Zn_2SnO_4 matrix. Similarly, the Ba-doped Zn_2SnO_4 gives an a-axis lattice constant of 8.679 Å. The substitution of smaller Zn^{2+} (0.74 Å) and Sn^{4+} (0.69 Å) cations with a much larger Sr^{2+} ion (1.18 Å) or Ba^{2+} (1.35 Å) should bring about an increase in cell volume and parameters, which could be verified by the observed slight peak shifts. The above evidences denote that the ternary oxide may be susceptible to doping considering the fact that the used dopants are much larger than those in ZTO lattice in ion radius.

As shown in Fig. 2, the morphologies and structures of three typical samples were characterized by TEM measurements. The images in Fig. 2a–f clearly show that the small doping amount of Sr^{2+} and Ba^{2+} cations has no obvious influence on the size and morphology of Zn_2SnO_4 nanoparticles, and all the samples display the spherical morphology with a diameter of 10–20 nm. According to the HRTEM images shown in Fig. 2 d–f, the lattice fringes with a spacing around 0.26 nm in all the samples can be ascribed to the (3 1 1) plane of ZTO. The diffraction rings in selected area electron diffraction (SAED) pattern